








Conceptual Design of 15 Tesla Conductor Test Facility for Future Fusion Reactor

Chao Dai , Yu Wu , Jinggang Qin , Yi Shi , Aihua Xu, Kaihong Wu, Yongliang Zhang , Xiaopeng Yu, Qiangwang Hao , and Arend Nijuis 

Abstract—“China Fusion Engineering Test Reactor (CFETR)” is a new generation of tokamak which aims to bridge the gaps between the fusion experimental reactor ITER and the demonstration reactor (DEMO). The superconducting magnet system is the core component in tokamak and future fusion reactor, and the superconducting magnet system for CFETR will be a big challenge due to the higher magnetic field is required. Based on the current design, the maximum field of Toroidal Field (TF) coil is around 14.5 T, and for Center Solenoid (CS) coil, the maximum field would be even higher. Now the significant work is developing high-performance Cable-in-Conduit Conductor (CICC) for these high field coils. Obviously, a test facility is necessary for developing new CICCs. It is well known that SULTAN facility plays an important and successful role in ITER conductor development, almost all ITER sample conductors were tested at SULTAN. But it’s hard to satisfy future test work due to its magnetic field limitation (<12 T). Now in China, a new program has been launched to build a new conductor test facility which has similar functions to SULTAN, but can provide background field up to 15 T. This paper will introduce the concept design of the magnet system of the superconducting conductor test facility.

Index Terms—CFETR, conductor test facility, split magnet, electro-magnetic design, conductor design.

I. INTRODUCTION

THE China Fusion Engineering Test Reactor (CFETR) is the next device in the roadmap for the realization of fusion energy in China, which aims to bridge the gaps between the fusion experimental reactor ITER and the demonstration reactor (DEMO) [1]. On the way to CFETR, several key issues should be preliminarily studied, one of them is the large scale and high-performance cable-in-conduit conductor (CICC). For example, according to the current design, CFETR TF coil would be a big

Manuscript received September 23, 2019; accepted February 14, 2020. Date of publication February 18, 2020; date of current version March 25, 2020. This work was supported in part by China Fusion Engineering Experimental Reactor General Integration and Engineering Design under Grant 2017YFE0300503 and in part by the Natural Science Foundation of the Jiangsu Higher Education Institutions of China under Grant 19KJB470011. (*Corresponding author: Chao Dai.*)

Chao Dai, Yu Wu, Jinggang Qin, Yi Shi, Xiaopeng Yu, and Qiangwang Hao are with the Institute of Plasma Physics, CAS, Hefei 230031, China (e-mail: qinjg@ipp.ac.cn).

Arend Nijuis is with the Energy, Materials and Systems, Faculty of Science and Technology, University of Twente, Enschede 7500AE, Netherlands.

Kaihong Wu and Yongliang Zhang are with the University of Sciences and Technology of China, Hefei 230026, China.

Aihua Xu is with the Changzhou Vocational Institute of Mechatronic Technology, Changzhou 213164, China.

Color versions of one or more of the figures in this article are available online at <http://ieeexplore.ieee.org>.

Digital Object Identifier 10.1109/TASC.2020.2974951

challenge, the maximum magnetic field is 14.5 Tesla, and the operating current is 95.6 kA. That means the Lorentz force on the conductor will be ~ 1400 kN/m, 1.5 times to ITER TF coil. Huge Lorentz force not only brings challenges to structural materials but also lead to another critical issue: conductor performance degradation [2], [3], [4]. ITER TF and early CS conductor suffered this problem due to Nb₃Sn filaments crack after EM and WUCD cycling under such high Lorentz force [3], [4]. Fortunately, the short twist pitch (STP) cable structure solved this problem effectively. In CFETR TF conductor development, STP structure will also be a good option, but the difference is that the high-performance Nb₃Sn strand will be used due to the performance of ITER type Nb₃Sn cannot satisfy the requirement of CFETR TF coil.

Although High-performance Nb₃Sn strand has been widely used in small cross-section CICC for high field magnet [5], [6], it is still challenging to apply this kind of strand into large cross-section CICC because it will suffer higher EM force and high-volume fraction of the brittle intermetallic phase in it makes it more sensitive to strain, so cable layout design is very important. Many efforts have been done to modeling the influence of cable layout to the strand performance under EM loading, but the effective way to verify the cable layout design is conductor performance test and a test facility is definitely needed. The well-known SULTAN facility plays an important and successful role in CICC development, but its maximum background field couldn’t satisfy the future CICC test mission. Here we report on a new project which aims to build a SULTAN-like test facility with the maximum background field up to 15 Tesla, the mission of this facility will be the performance study of future high field CICC for CFETR and DEMOs worldwide. In addition, this test facility will provide a large space, high magnetic field environment for other researches.

II. MAGNET DESIGN OVERVIEW

The magnet system is the key component of the test facility, which consists of three split pairs of the solenoid coil, and they are named to be inner coil (IC), middle coil (MC), outer coil (OC) based on their positions respectively. The design criterion requires that the magnetic field deviation on the test sample should be below 2% within the length of 550 mm. All the coils are wound by three different rectangular Cable-In-Conduit Conductor (CICC) layouts (see the Section IV) with different types of Nb₃Sn strand. For inner coils and middle coils, High-performance Nb₃Sn strand will be used for outer coils, the Nb₃Sn strand which is used for CFETR CSMC will be used. The strand performances are introduced in Section III. After optimizations, six coils are divided into two groups by two power

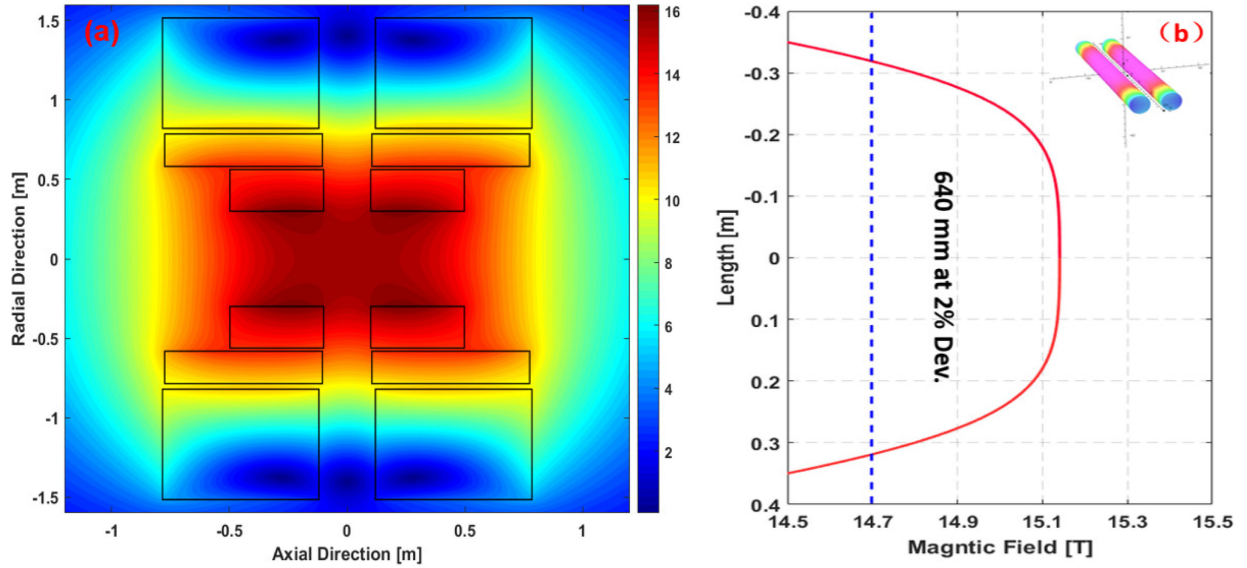


Fig. 1. (a) Magnetic field distribution of the magnet. (b) Magnetic field distribution in longitude direction on the test sample.

TABLE I
THE OPERATING PARAMETERS OF THE MAGNET

	IC1&IC2	MC1&MC2	OC1&OC2
Operating current [kA]	8.0	8.0	13.5
Maximum field [T]	15.75	13.3	10.5
Operating temperature [K]	4.5	4.5	4.5

TABLE II
THE INDUCTANCE MATRIX OF THE MAGNET

	IC1	IC2	MC1	MC2	OC1	OC2
IC1	0.0222	0.0047	0.029	0.0094	0.05	0.028
IC2	0.0047	0.0222	0.0094	0.029	0.028	0.05
MC1	0.029	0.0094	0.106	0.0241	0.21	0.088
MC2	0.0094	0.029	0.0241	0.106	0.088	0.21
OC1	0.05	0.028	0.21	0.088	1.28	0.47
OC2	0.028	0.05	0.088	0.21	0.47	1.28

supplies, inner and middle coils are with one power supply and outer coils are with one power supply, which can maximize the strand performance and make the magnet more compact. The magnetic field distribution of the magnet is shown in Fig. 1(a), and Fig. 1(b) shows the field profile on the 550 mm length test sample. The operating parameters are listed in Table I, and the inductance matrix is shown in Table II, the total inductance is about 5.5 H and the stored magnetic energy is estimated to be ~ 410 MJ. The 2-D structure analysis has been done, result shows that the maximum Tresca stress is 574 MPa and located on the jacket of inner coil, which is shown in Fig. 2(a). The Tresca stress is within the allowable stress criteria ($2/3$ times yield stress) of modified 316LN. The 3-D structure analysis, which takes the thermal contraction and pre-load into consideration is ongoing, the results would be presented in future article.

Fig. 2(b) shows the structure of the magnet. The winding method for inner and middle coils is layer wound, and the winding method for outer coils is a double pancake. The minimum

distance of the gap between the split coils is 200 mm. Take the volume of the structural components into consideration, the dimension of the room temperature aperture for a SULTAN-like U-shaped conductor test sample is 160×100 mm. The maximum field on the sample will be ~ 16.5 Tesla if the self-field is considered. The inner diameter of the magnet is 600 mm, which could provide a high magnetic field environment for other experiments in the future.

III. THE SUPERCONDUCTING STRAND

Since the maximum field of the inner coils is higher than 15 T, the high- J_c Nb₃Sn strand should be taken into consideration. For mid coils, their maximum field is 13.3 T, that means high-performance Nb₃Sn strand and ITER-grade Nb₃Sn strand are both adaptable. But using high-performance Nb₃Sn strand can reduce the number of superconducting strand and coil volume, meanwhile increases the number of cooper strand in the cable, which can improve the conductor stability and reduce the hot spot temperature when the quench happens (the analysis is in Section IV). The maximum magnetic field of outer coils is 10.5 T, that means ITER grade Nb₃Sn is adequate.

At present, several companies are developing high-performance Nb₃Sn strand, including Bruker-OST, WST, Lu-vata *et al.* For this project, one of the most important requirements to strand is performance stability, which means the maturity and industrialization of the strand should be cited as the first priority. The OST restacked-rod-process (RRP) Nb₃Sn strand has been developed for more than ten years and adopted in some facilities, such as EDIPO and China 40 T hybrid magnet outsert [7], [8]. In the conceptual design, the performance of RRP strand was used to do the calculation and analysis.

The performances of two kinds of RRP strand, OST-M2007 ($J_c > 2200$ A/mm² at 12 T, 4.2 K) and OST-E2013 ($J_c > 2700$ A/mm² at 12 T, 4.2 K), were evaluated by experiments. The $J_c(B, T, \varepsilon)$ tests were performed at University of Geneva and University of Twente. Fig. 3 shows the comparison of the critical current density versus strain between two kinds of the strand at

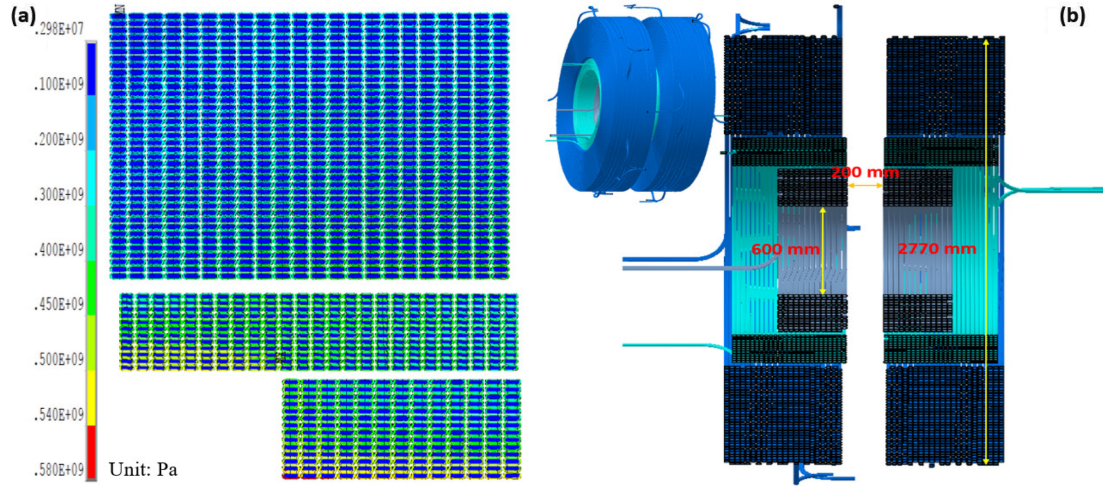


Fig. 2. (a) The Tresca stress distribution on the coils. (b) The coils geometry and main dimensions.

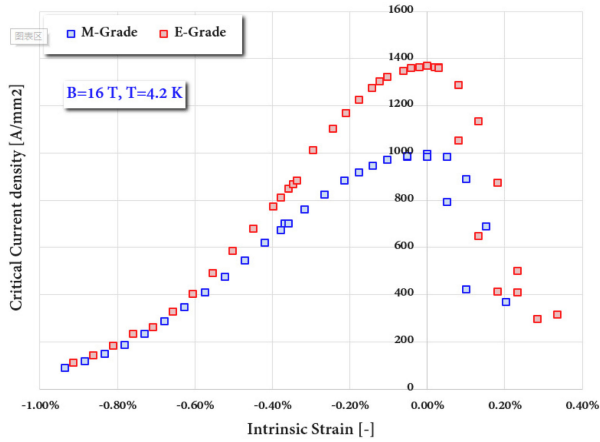


Fig. 3. Comparison of the strain dependence critical current density of OST M2007 strand and E2013 strand at 16 T and 4.2 K.

16 T, 4.2 K. It can be seen that at high strain region ($\epsilon > -0.5\%$), the critical current density of M2007 strand is close to that of E2013. Obviously, M2007 has higher cost performance. The Nb_3Sn strand for CFETR CSMC is from WST, its $J_c(B, T, \epsilon)$ have been tested with PACMAN at UT and ASIPP. The test results of these two types of Nb_3Sn strand were fitted with the deviatoric model [9], and the fitting parameters are listed in Table III. In the following section, the CICC design is based on the performances of ITER-grade Nb_3Sn strand and OST M2007 RRP Nb_3Sn strand.

IV. THE CABLE-IN-CONDUIT CONDUCTOR DESIGN

For a large aperture and high magnetic field magnet, the cable-in-conduit conductor is the best choice, due to its high current carrying capacity, high mechanical strength, and high stability. Referring to other magnets with similar scale [5], [6], the CICC consists of 4 stages of sub-cable without central cooling channel is appropriate for this magnet. The key criteria are the temperature margin and the hot spot temperature during discharging. The temperature margin is set to be 1.2 K, which means the current sharing temperature T_{CS} should be higher than 5.7 K. The hot

TABLE III
THE FITTING PARAMETERS OF TWO KINDS OF Nb_3Sn STRAND

	OST M2007 Nb_3Sn	CSMC Nb_3Sn
$Ca1$	49.00	38.00
$Ca2$	0.300	2.60
$\epsilon_{0,a}(\%)$	0.312%	0.240%
$\epsilon_m(\%)$	-0.059%	-0.407%
$\mu_0 H_{c2m}(0) (T)$	33.24	29.17
$T_{cm}(0) (K)$	16.34	15.92
$CI (A T)$	21700	47700
p	0.593	0.5
q	2.156	2.0

TABLE IV
THE OPERATING PARAMETERS OF THE MAGNET

	Inner coil	Middle coil	Outer coil
Strand	OST M-grade Nb_3Sn ($d=0.81$ mm with Cr plated)		Nb_3Sn strand for CFETR CSMC ($d=0.82$ mm with Cr plated)
Cu: Non-Cu	1.0	1.0	1.0
RRR	100	100	100
Cable Pattern	3sc \times 4 \times 5 \times 6	(1sc+2cu) \times 4 \times 4 \times 5	(1sc+2cu) \times 4 \times 5 \times 6
Number of SC	360	80	120
Number of Cu	0	160	240
Void Fraction (%)	~32	~32	~32
Jacket thickness (mm)	2.2	2.2	2.2
Insulation	1.0mm S-glass fiber tape		

spot temperature should be below 250 K with adiabatic model calculation and below 150 K with thermal-hydraulic simulation [10]. According to present design, heat-treatment followed by insulation will be adopted for all coils, that means the Kapton layer will be absent in the insulator, then the coil maximum discharge voltage is limited to 2 kV. The preliminary designed conductor parameters are listed in Table IV.

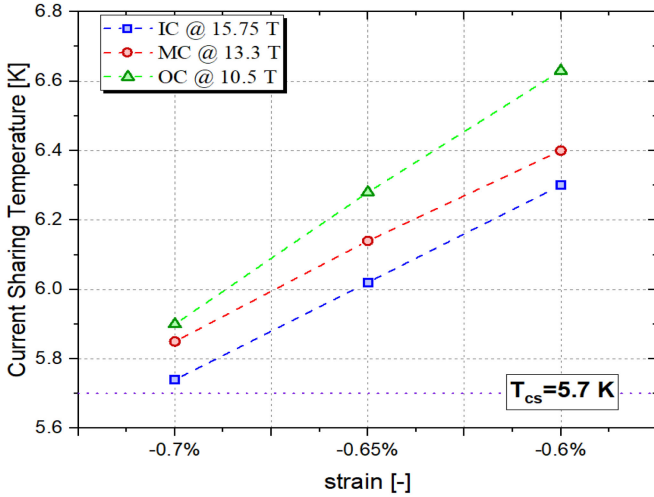


Fig. 4. Current sharing temperatures assessment of three conductors under various effective strain.

Based on the operating parameters listed in Table I, and the cable patterns in Table IV, the T_{cs} of each conductor can be estimated. Referring to the EDIPO conductor test results [5], the effective strain is assumed to be -0.65% , which is a relatively conservative value. Fig. 4 shows the current sharing temperatures of the three conductors, with the effective strain from -0.6% to -0.7% . From the figure, it can be seen that the current sharing temperatures of three conductors can satisfy the criteria, the inner coil conductor has a degradation margin of 0.32 K at the effective strain of -0.65% .

At the initial stage of the design work, the discharge time constants of the two groups of coils are conservatively estimated by the adiabatic model [11]:

$$\frac{I_{op}^2}{A_{cu}^2} t_d + \int_0^\infty \frac{I(t)^2}{A_{cu}^2} dt = J_0^2 t_d + K = Z(T_f)$$

Where I_0 is the initial current, t_d is the quench detection delay time. By this simple approach, the initial discharge time constants for two groups of coils can be estimated to satisfy the conductor hot spot temperature criterion. The initial discharge time constants are 30 s for outer coils and 23 s for inner and mid coils. But this magnet system is driven by two power supplies, which means there two circuits and inter-coil coupling should be taken into consideration. The current decay of the inductively coupled system could be solved by an ODEs system:

$$\begin{pmatrix} L_{11} & \dots & M_{1n} \\ \vdots & \ddots & \vdots \\ M_{m1} & \dots & L_{nn} \end{pmatrix} \cdot \begin{bmatrix} dI_1/dt \\ \vdots \\ dI_n/dt \end{bmatrix} + \begin{pmatrix} R_1 & \dots & 0 \\ \vdots & \ddots & \vdots \\ 0 & \dots & R_n \end{pmatrix} \times \begin{bmatrix} I_1 \\ \vdots \\ I_n \end{bmatrix} = 0$$

where L is the inductance, M is the mutual inductance, I is current, and R is the quench protection resistor. It assumes that the two circuits discharge synchronously, and the protection resistors are calculated with the time constants from adiabatic model. Then the current decay ODEs can be solved and the

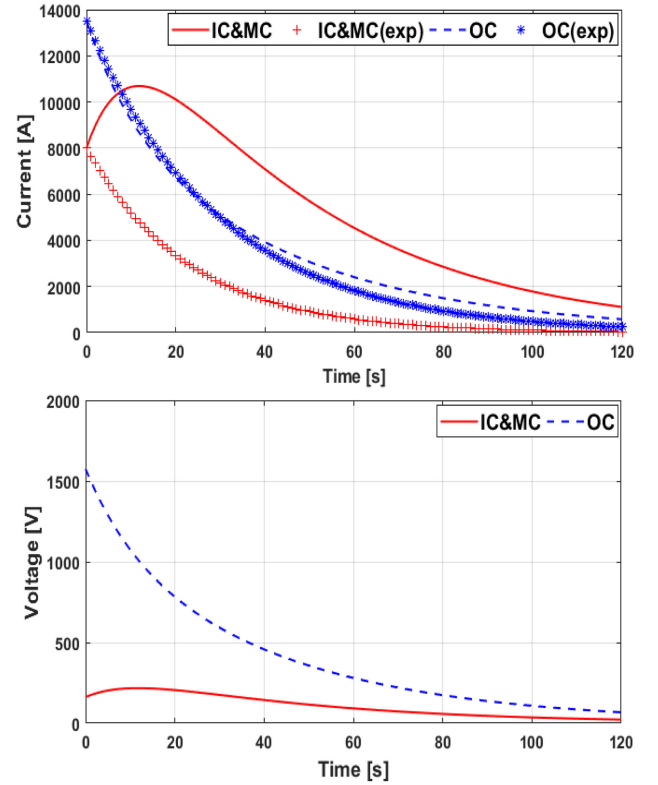


Fig. 5. Current and voltage curves of coils during discharge before optimization.

results are plotted in Fig. 5. It can be seen that a big current is induced on inner-mid coil circuit by outer coil circuit due to the inductance of outer coils is much higher than inner and mid coils. After recalculating the hot spot temperature with the current decay curve considering the coupling, the results show that the hot spot temperature of IC-MC conductor exceeds the criterion due to extra energy is released on the conductor.

For suppressing the inductive current on inner & mid coils during discharge, the quench protection resistor of outer coil and inner-mid coils are changed from 0.1337Ω and 0.0203Ω to 0.1556Ω and 0.0513Ω . The optimized results are shown in Fig. 6, the calculation results indicate that the hot spot temperatures of inner-mid coil conductor and outer coil conductor are below 250 K, and the coil discharge voltages of the two circuits are below 2 kV.

Thermohydraulic simulations of quench were carried out with GANDALF code [12]. The simulation length of the conductor was chosen to be 300 m, which is an average value for the cooling channel. The boundary conditions are assuming the inlet temperature of 4.5 K and pressure of 5 bar. The helium mass flow rate is 2 g/s. The current decay curves in Fig. 6 and the effective strain of -0.65% are inputted into the simulation. The maximum temperatures and maximum pressures as functions of time are plotted with scatters and lines respectively in Fig. 7. It can be seen that the maximum temperatures of each conductor with different quench detection delay times are below 150 K, which is within the criterion of thermal-hydraulic simulation. The maximum internal pressure is 1.58 MPa for the mid coil conductor, and the mechanical analysis shows that maximum Tresca stress on the jacket caused by the internal pressure is 54 MPa, located in the inner corner of the jacket. It is below

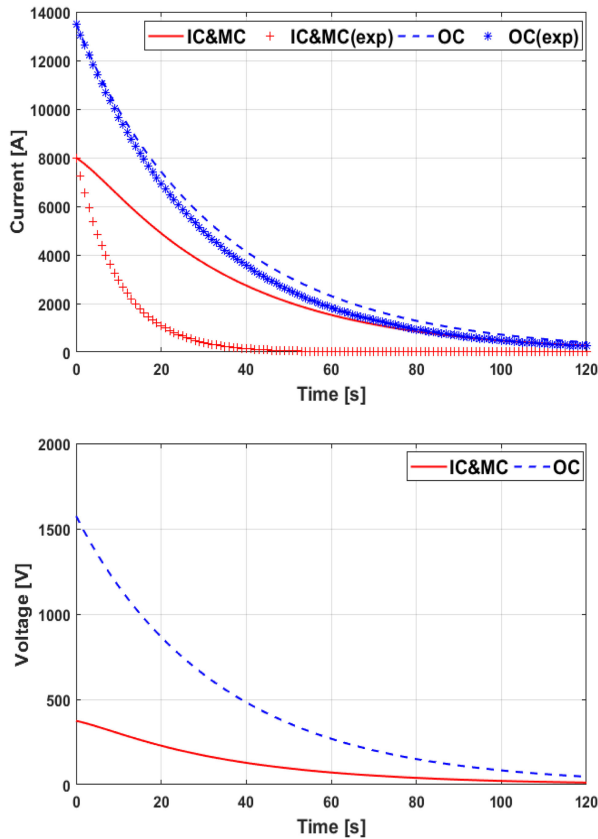


Fig. 6. Current and voltage curves of coils during discharge after optimization.

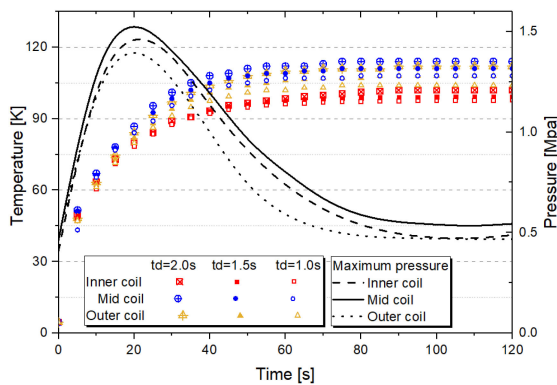


Fig. 7. The hot spot temperatures and maximum pressure of three coils simulated with GANDALF code vary as a function of time.

the allowable stress criteria of 316LN, which means the 2.2 mm jacket thickness is safe.

In future work, further analysis needs to be carried out. For example, the Lorentz force should be assessed and the

jacket thickness of the conductor may need adjustment. AC loss assessment of the conductors will be initiated and conductor samples should be prepared for SULTAN test. The conductor structures, like the twist pitch, conductor geometry, etc. will be optimized based on this further analysis. Also, the design work of the structural components of the magnet like supports, Dewar, thermal shield, etc. is ongoing.

V. SUMMARY

The 15 Tesla conductor test facility is a fundamental facility for the CFETR program. The main mission of this facility is providing the various test conditions for future high-performance, large-scale superconductors. At present, the conceptual design of its magnet system is completed, which consists of three concentric split pairs of Nb₃Sn coil.

In parallel with the magnet system design, preliminary work of other auxiliary systems, such as power supplier system, cryogenic system, and quench protection system have been carried on.

As the most significant component of the magnet, the parameters of the prototype conductors will be solidified and the conductor short samples will be manufactured and tested in the next stage of work.

REFERENCES

- [1] W. Yuanxi *et al.*, "Overview of the present progress and activities on the CFETR," *Nuclear Fusion*, vol. 57, no. 10, 2017, Art. no. 102009.
- [2] M. Breschi *et al.*, "Results of the TF conductor performance qualification samples for the ITER project," *Supercond. Sci. Technol.*, vol. 25, no. 9, 2012, Art. no. 095004.
- [3] A. Devred *et al.*, "Challenges and status of ITER conductor production," *Supercond. Sci. Technol.*, vol. 27, no. 4, 2014, Art. no. 044001.
- [4] S. Carlos *et al.*, "Metallographic autopsies of full-scale ITER prototype cable-in-conduit conductors after full cyclic testing in SULTAN: 1. The mechanical role of copper strands in a CICC," *Supercond. Sci. Technol.*, vol. 28, no. 8, 2015, Art. no. 085005.
- [5] A. Vostner *et al.*, "Development of the EFDA dipole high field conductor," *IEEE Trans. Appl. Supercond.*, vol. 18, no. 2, pp. 544–547, Jun. 2008.
- [6] Y. F. Tan *et al.*, "The design of cable-in-conduit conductors for the superconducting outsert coils of a 40 T hybrid magnet," *Supercond. Sci. Technol.*, vol. 22, no. 2, Feb. 2009, Art. no. 025010.
- [7] W. G. Chen *et al.*, "Final design of the 40 T hybrid magnet superconducting outsert," *IEEE Trans. Appl. Supercond.*, vol. 23, no. 3, Jun. 2013, Art. no. 4300404.
- [8] A. Portone *et al.*, "Status report of the EDIPO project," *IEEE Trans. Appl. Supercond.*, vol. 21, no. 3, pp. 1953–1959, Jun. 2011.
- [9] A. Nijhuis, Y. Ilyin, and W. Abbas, "Axial and transverse stress-strain characterization of the EU dipole high current density Nb₃Sn strand," *Supercond. Sci. Technol.*, vol. 21, no. 6, 2008, Art. no. 065001.
- [10] ITER Design Description Document: DDD 11 ITER_D_2NBKXY, "Magnets-7-Conductor" v1.2, Sep. 09, 2009.
- [11] Y. Iwasa, *Case Studies in Superconducting Magnets-Design and Operational Issues*, 2nd ed. New York, NY, USA: Plenum, 2009, pp. 471–479.
- [12] "GANDALF: A Computer code for quench analysis of dual flow CICC's," [Online]. Available: <http://botturl.web.cern.ch/botturl/CryoSoft/gandalf.html>